



# Electron paramagnetic resonance monitoring for on-demand electrochemically-generated radicals



Mohamed A. Morsy<sup>a,\*</sup>, Abdel-Nasser M. Kawde<sup>a,b</sup>

<sup>a</sup> Chemistry Department, College of Sciences, King Fahd University of Petroleum and Minerals, Dhahran 31261, Saudi Arabia

<sup>b</sup> Chemistry Department, Faculty of Science, Assiut University, Assiut, 71516, Egypt

## ARTICLE INFO

### Article history:

Received 15 December 2014

Received in revised form 29 January 2015

Accepted 2 February 2015

Available online 4 February 2015

### Keywords:

Electron Paramagnetic Resonance

Electrochemistry

Drug Analysis

Graphite Electrode

Radicals

Ketoconazole

## ABSTRACT

An in-situ electrochemical–electron paramagnetic resonance (EC–EPR) spectroscopy techniques utilizing a new inexpensive and disposable two-electrode system cell was developed. The EC–EPR cell provided maximal sensitivity, minimal dielectric loss along the central axis of the EPR cavity, and was easy handled/mounted without the need for additional adjustments. The developed method was utilized for the analytical determination of ketoconazole (KTZ). The process relied on monitoring the peak-to-peak EPR signal intensities obtained from KTZ radical species that were generated electrochemically at disposable graphite pencil electrode (GPE) surfaces. Optimization of the EC–EPR parameters enabled KTZ radical detection at a concentration and with a volume that were one order of magnitude lower than the corresponding concentrations and volumes tested using chemical oxidation analysis techniques. Moreover, ‘on-demand’ radical formation was achieved by alternating the applied potentials between the ‘ON’ and ‘OFF’ that was used to explore the kinetic of the KTZ-oxidation and its oxidative products.

© 2015 Elsevier Ltd. All rights reserved.

## 1. Introduction

Spectroscopic techniques, such as X-ray [1–5], infrared (IR) and Raman [6–9], UV–vis [10–12], nuclear magnetic resonance (NMR) [13–15], and EPR [16–19] spectroscopies are versatile tools for chemical analysis, particularly in the pharmaceutical and biopharmaceutical fields. Many of these spectroscopic techniques are routinely utilized in drug applications, such as characterizing formulations or elucidating the kinetic processes associated with drug delivery. The techniques are officially included in United States Pharmacopeia (USP) [20]. EC-methods, such as cyclic, square wave, normal, and differential pulse voltammetry, may be applied at unmodified or modified electrode surfaces for the analysis of drug formulations [21–23]. These methods are simple, low-cost, and highly sensitive for analyzing drugs in pharmaceutical formulations, and in human body fluids compare to other routine analytical techniques [24–28].

More than fifty years ago, a simultaneous EC–EPR technique was developed to gain insight into the identity and reactivity of paramagnetic species [29]. The method has been accepted as a highly powerful mean for identifying paramagnetic intermediates in EC-reactions [30]. A variety of EC–EPR cells have been designed to facilitate this technique [31]. However, these cells are either

expensive or not easy to use, and the electrodes in these cells are made of platinum or silver precious metals. Moreover, these various EC-cell designs could not be utilized for the EC–EPR redox processes on the surface of graphite electrodes.

The present work uses a simple, inexpensive EC–EPR cell for the determination of KTZ. Unlike our recently reported chemical oxidation of the acidified KTZ by Ce(IV) [18], the current EC-oxidation relies on the radicals’ formation rather than disappearance, which enables the ‘on-demand’ formation of radicals at disposable graphite pencil electrode (GPE) surfaces by alternating the applied potential between ‘ON’ and ‘OFF’ states. It is also used to elucidate the kinetic of the acidified KTZ oxidation and to identify its oxidative products that could be linked to its delivery in acidic solutions.

## 2. Experimental

### 2.1. Reagents

Analytical grade KTZ and the Cu, Ag, and Pt pure metals were purchased from Sigma–Aldrich, USA. H<sub>2</sub>SO<sub>4</sub> was purchased from Merck, UK. The pencil leads were obtained from Pentel Co. Ltd. Japan, Faber–Castell, Ohio, USA, and LYRA, Selangor, Malaysia, and were named high-polymer Super C505 (Black lead) of types HB, B, and H. All leads had a total length of 60 mm and a diameter of 0.3 or 0.5 mm, and were used as received. Acidified double-distilled

\* Corresponding author. Tel.: +966 13 860 4761; fax: +966 13 860 4277  
E-mail address: [mamorsy@kfupm.edu.sa](mailto:mamorsy@kfupm.edu.sa) (M.A. Morsy).

water containing  $0.1 \text{ mol dm}^{-3} \text{ H}_2\text{SO}_4$  was used throughout the preparation and dilution of the KTZ solutions.

## 2.2. Instrumentation

A CHI-1220 (CH instruments Inc. Austin, Texas, USA) potentiostat combined with a MiniScope MS300 EPR spectrometer (Magnettech GmbH, Germany), upgraded with an ADANI CMS8400's frequency meter and a fast registry operated at the CW X-band and equipped with a two-electrode EC-cell (Fig. 1) was utilized to monitor the EC and EPR outputs of the instantaneously generated radicals via EC-redox reactions.

The two-electrode system EC-disposable cell consisted of an Ag/AgCl auxiliary electrode (AUX), and a working electrode (WE) made of either copper, silver, platinum or graphite materials. A schematic diagram of the cell components and their assembled sketch is shown in Fig. S1 of the *Supplementary Information*. Both AUX and WE electrodes were tightly placed in a disposable glass capillary tube filled with an acidified KTZ solution. Then, the disposable cell is housed in a non-disposable 3 mm EPR quartz tube as a cell holder. A detailed description, fabrication and utilization of the proposed cell is presented in a recently filed discloser at the United States Patent of Trademark Office (USPTO) [32].

Working electrodes' surfaces were investigated and analyzed using JEOL JSM-6610 LV-scanning electron microscopy (SEM) equipped with an energy-dispersive X-ray spectroscopy Unit (JEOL EDS) and an acceleration voltage up to 20 keV. All precious metal and graphite pencil samples were directly mounted on a carbon film without pre-treatment or coating.

## 3. Results and Discussion

Fig. 2A shows the EPR spectra obtained from KTZ radicals produced at different WE surfaces in the proposed cell. Indistinguishable EPR signals were obtained from the Cu- and Ag-metal electrode surfaces and relatively very weak response was obtained from the Pt electrode. A similar weak response has been obtained by using a two-electrode conventional-electrolysis suprasil flat cell (Wilmad WG-812-Q, Ag/AgCl electrode (AUX), and 0.1 mm Pt-wire electrode (WE)) that has a 0.3 mm space.

Much stronger EPR intensities were found at various graphite pencil surfaces (Fig. 2A and inset) as WE in the current simple cell. The HB-graded graphite pencils (HB-GP) showed three to ten times the produced of radicals observed on the B or H graphite or by the Pt surfaces, in a given  $50 \mu\text{g mdm}^{-3}$  (ppm) acidified KTZ solution (Fig. 2B). These results on HB-GP are consistent with early EC-measurements collected at a variety of graphite pencil electrodes [33] and with present cyclic voltammograms (CVs) responses of different WEs shown in Table S1 of the *Supplementary Information*. The geometry of the available conventional-electrolysis flat cell would not allow to test any of the graphite pencil WEs, even the smallest 0.3 mm commercially available one.

The differences in radical concentrations generated at different WE surfaces could be explained in terms of the surface morphology, as the EC-reactions result from interfacial phenomena, which directly influenced the number of analyte molecules adsorbed onto the surface and the immovability of the produced intermediate(s). The SEM images presented in the inset of Fig. 2B indicate marked differences in the surface roughness properties of the Pt and the graphite electrodes. The later formed stacks of compressed platelets whereas the Pt electrode showed a smooth surface. The rough surface yielded a larger surface area, a higher affinity for the analyte [34–37], and stronger adsorption of the analyte.

Similarities between the SEM images obtained from the HB-grade electrode (inset of Fig. 2B) and the other graphite electrode surfaces (data not shown) indicated that variations in the composition, as observed in the EDS results, contributed to the observed minor EPR response differences, rather than differences in the surface morphology. Earlier investigations indicated that the ferromagnetic properties of graphite materials vary as a function of the interfacial disorder due to higher levels of clay (mainly  $\text{SiO}_2$  and a small amount of metal oxides) in the matrix [38–40]. Among the different graphite types examined in the present studies, the HB-GP was least able to control the magnetization ratio ( $M_R/M_S$ ) and the coercivity ( $H_C$ ), where  $M_R$  indicates the remnant magnetization or magnetization retained after reducing the field,  $M_S$  indicates the spontaneous magnetization, and  $H_C$  indicates the negative magnetic field needed to reduce the remnant magnetization [41]. Thus, the weak magnetic properties and little heterogeneity in the HB-GP material provided optimal surface properties for promoting the EC-processes required to produce the observed maximum possible electro-redox intermediate species.

The time-dependent peak-to-peak intensities corresponding to the KTZ-radical intermediates are shown in Fig. 2B and indicated that the electro-oxidation radical production processes initiated by KTZ followed by a series of sequential reactions as shown in Scheme 1, in which a series of first-order reactions generates, via oxidation, the KTZ-radical intermediate(s)  $[\text{KTZ}]^+$ . Thus, the time-dependent radical intermediate concentration over the reaction time ( $t$ ) and the value  $t_{\text{max}}$  (the time at which  $[\text{KTZ}]^+$  reached a maximum or  $([\text{KTZ}]^+)_{t=t_{\text{max}}}$ ) are given by Eq. (1) and Eq. (2) [42].

$$[\text{KTZ}]_t^+ = \frac{k_1}{k_z - k_1} (e^{-k_1 t} - e^{-k_z t}) [\text{KTZ}]_0 \dots \dots \dots (1)$$

$$t_{\text{max}} = \frac{1}{k_1 - k_z} \ln \left( \frac{k_1}{k_z} \right) \dots \dots \dots (2)$$

The gradual increase in the concentration and observed  $t_{\text{max}}$  for this intermediate showed that the rates at which the radical intermediate formed and decayed were comparable. The estimated rate constant values were  $10^{-3} \text{ s}^{-1}$ , in agreement with the

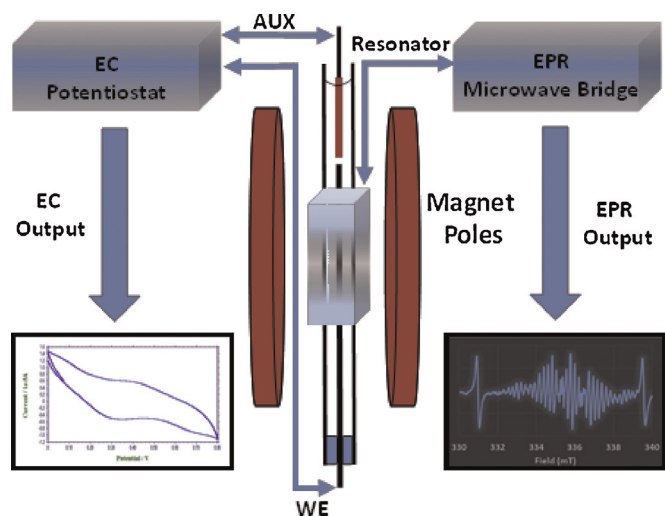


Fig. 1. Schematic illustration of the EC-EPR setup, including an EC potentiostat, an EPR spectrometer, the disposable part of the proposed EC-EPR cell, and the corresponding outputs obtained from the 50 ppm acidified KTZ solution.

Download English Version:

<https://daneshyari.com/en/article/184382>

Download Persian Version:

<https://daneshyari.com/article/184382>

[Daneshyari.com](https://daneshyari.com)